

iScience, Volume 23

Supplemental Information

rs953413 Regulates Polyunsaturated Fatty Acid Metabolism by Modulating *ELOVL2* Expression

Gang Pan, Marco Cavalli, Björn Carlsson, Stanko Skrtic, Chanchal Kumar, and Claes Wadelius

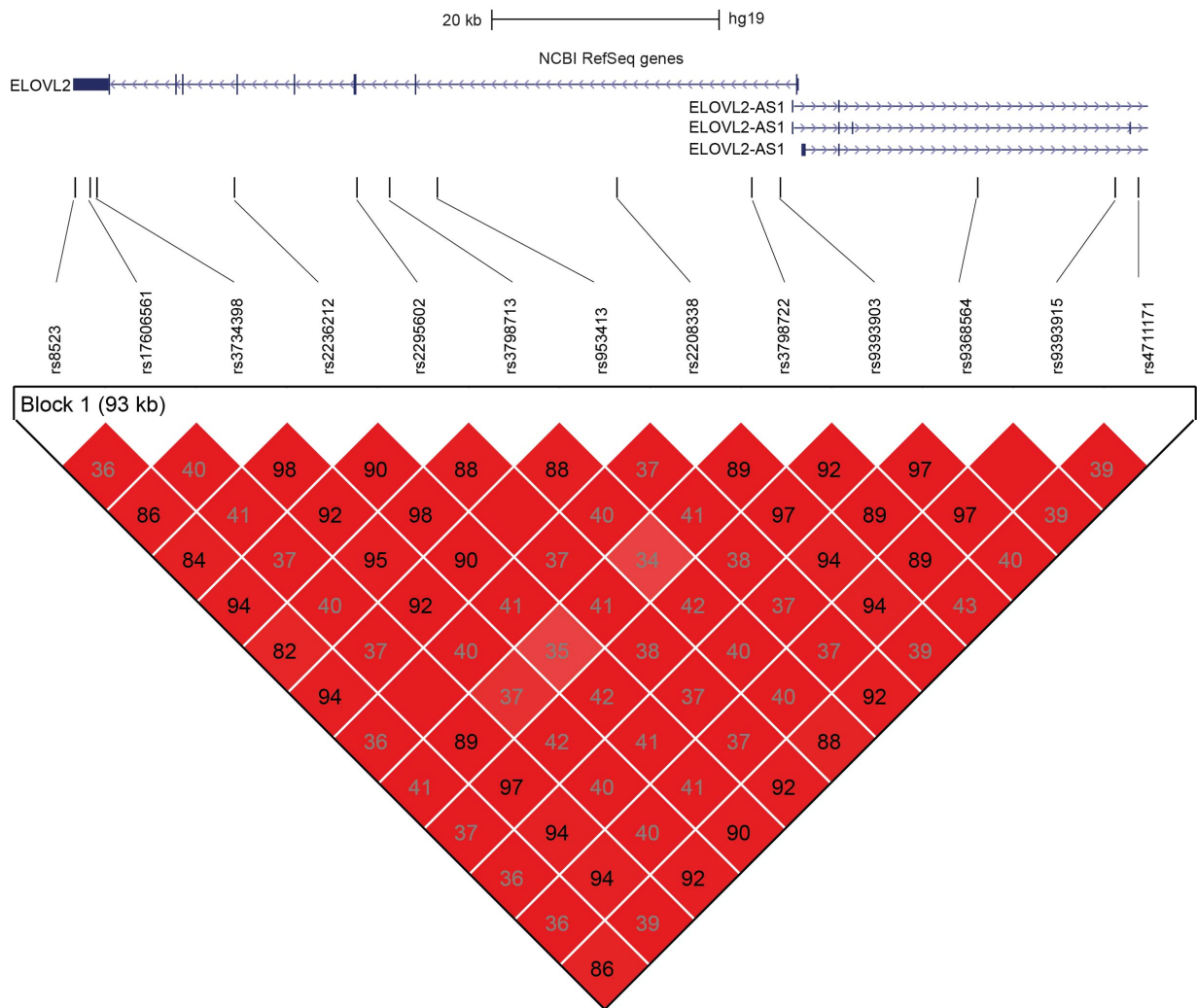


Figure S1. The reported tag SNPs in the *ELOVL2* locus associated with LC-PUFAs derived metabolites in GWAS are in high LD. Related to Figure 1. The tag SNPs are from the GWAS listed in Table S1. The color in each well denotes LOD value while the number denotes r^2 value between pair of SNPs in European population (CEU in 1000 Genomes Phase 3).

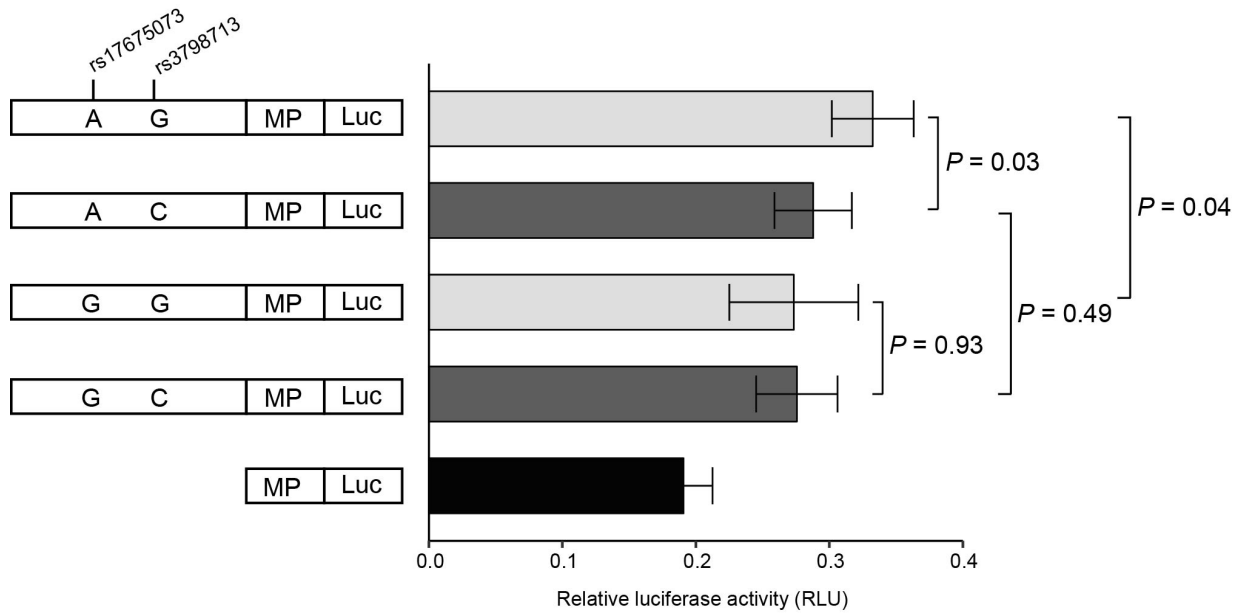


Figure S2. Luciferase assay on the rs3798713 region. Related to Figure 1. Both rs3798713 and rs17675073 are AS-SNPs in HepG2 cells that are in proximity. To evaluate the effect of each SNP, luciferase constructs containing different genotypes were constructed by direct PCR and site-directed mutagen with primers listed in Table S4. Error bars, s.d. $n = 6$ from two independent plasmid extractions and transfections with each transfection had three technical replicates. P values were calculated using two-tailed Student's t tests.

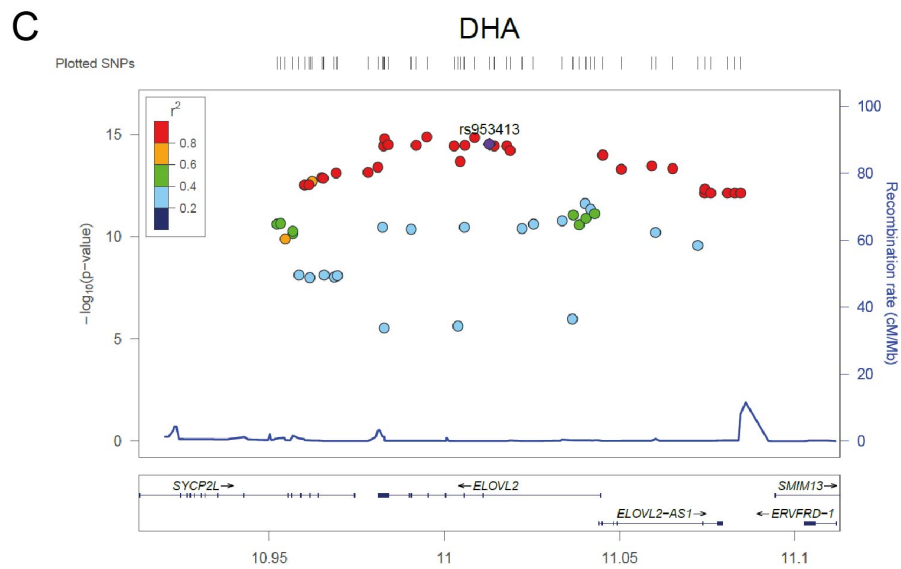
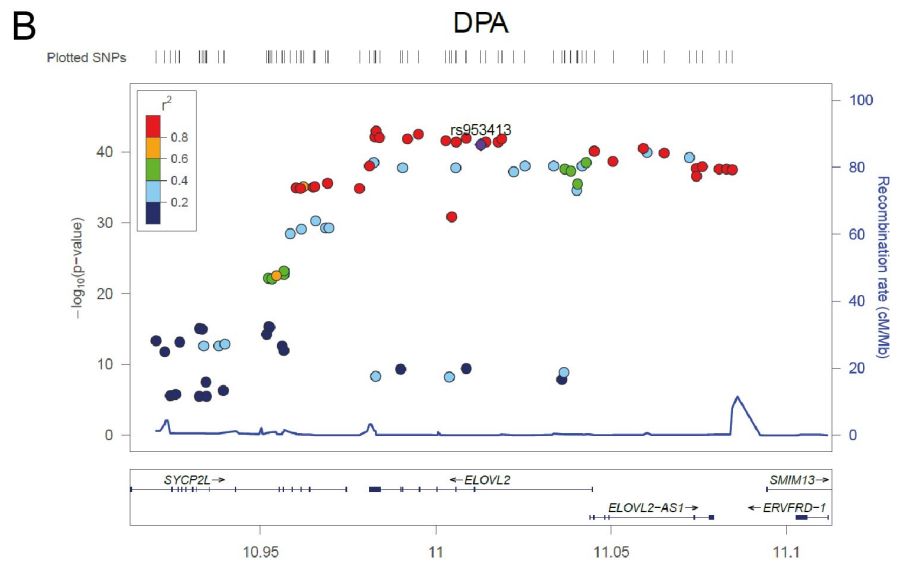
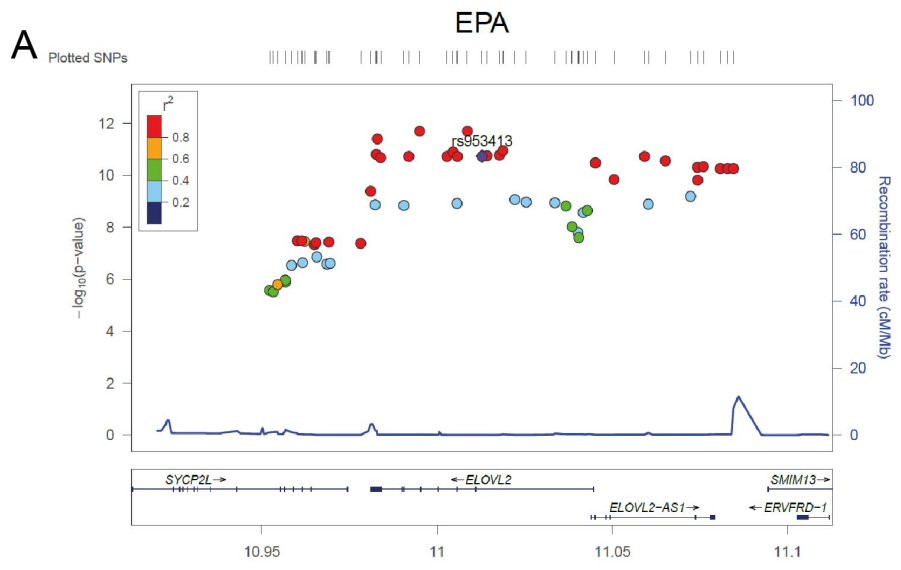


Figure S3. rs953413 and its proxies showed more statistical powder in associating with levels of ω -3 fatty acids in plasma phospholipid. Related to Figure 1. All the significant SNPs in the *ELOVL2* locus associated with EPA (A), DPA (B) and DHA (C) in the meta-analysis carried out in the CHARGE Consortium were plotted (Lemaitre et al., 2011). The plots were generated with rs953413 as the reference and LD is indicated by color scale in relation to rs953413 (r^2 values calculated in EUR in 1000 Genomes Phase 3).

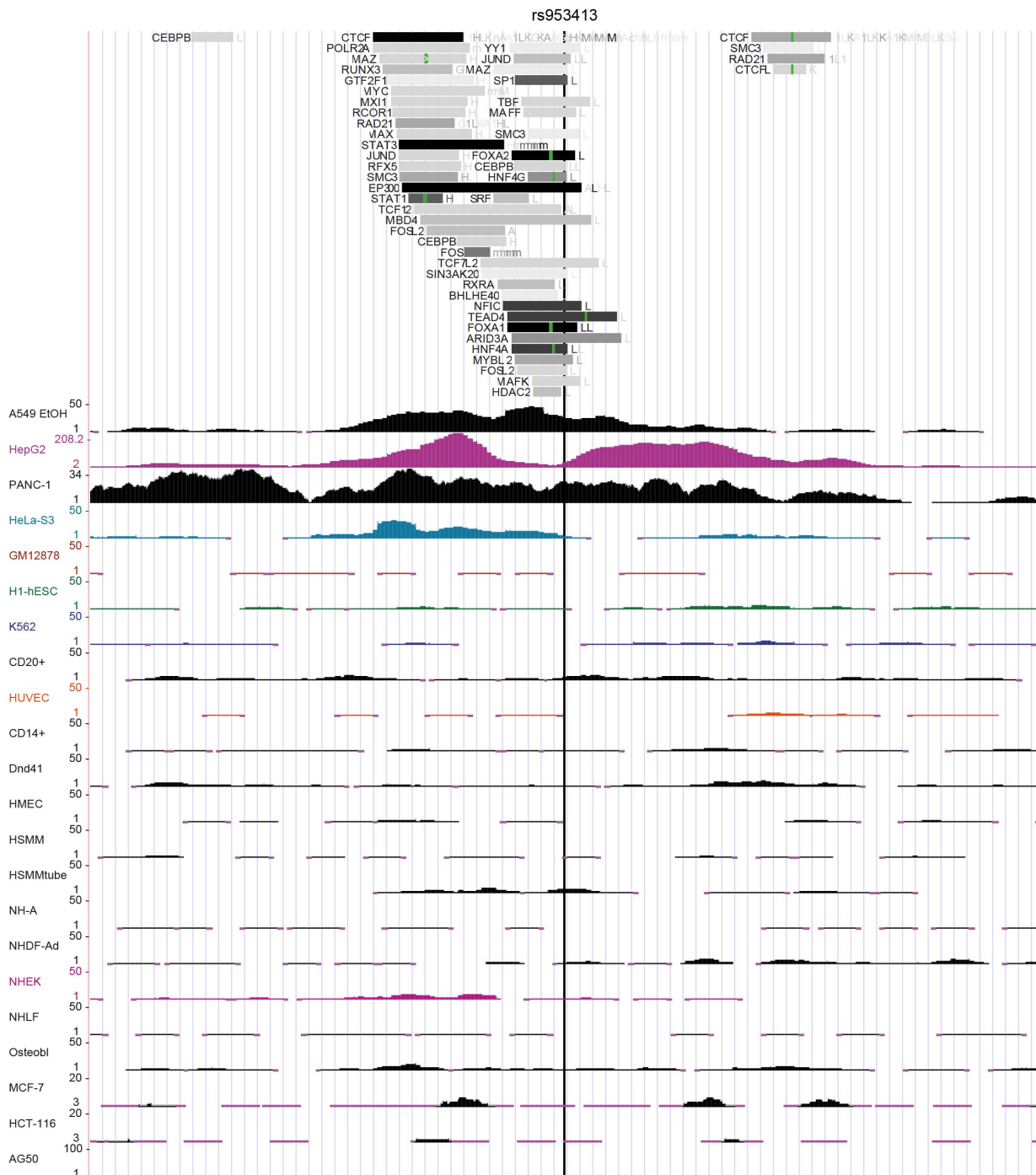


Figure S4. rs953413 is located in a liver-specific enhancer region. Related to Figure 1. A 5-kb window with rs953413 in the center is displayed here. The H3K27ac signals in HepG2 and other cell lines from the ENCODE project are shown for this region (The Encode Project Consortium, 2012). The exact location of rs953413 is highlighted by a vertical black line. The rs953413-containing region is also bound by many TFs in the liver which is identified by ChIP-seq experiments with antibodies against different TFs from the ENCODE project and is shown at the top.

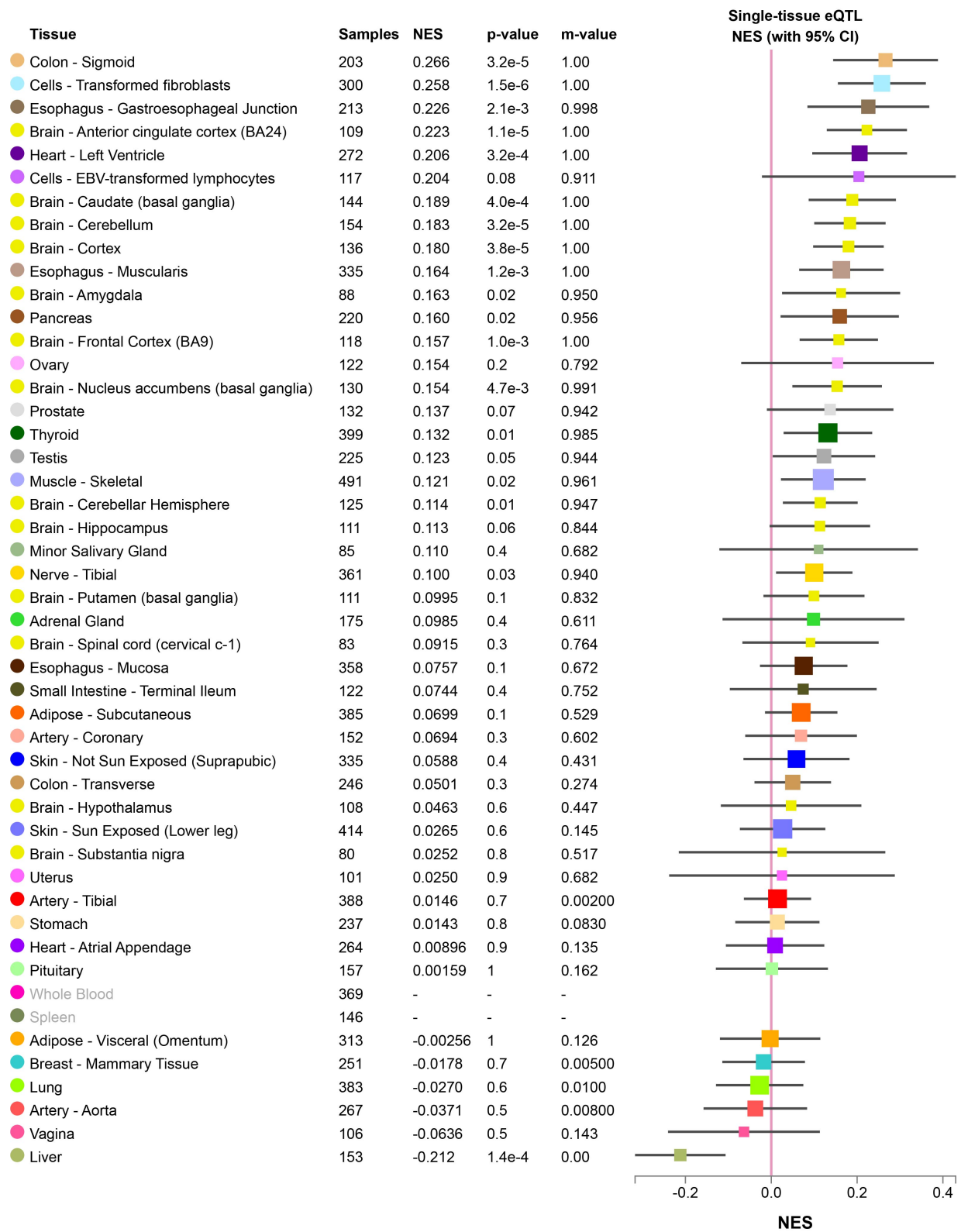


Figure S5. The eQTL analysis of rs953413 on *ELOVL2* expression in multiple tissues from the GTEx portal. Related to Figure 1. The figure was directly downloaded from the GTEx portal with minor modifications (Battle et al., 2017). NES, normalized effect size. In the liver tissue, the A allele of rs953413 is associated with decreased expression of *ELOVL2* with NES of -0.212.

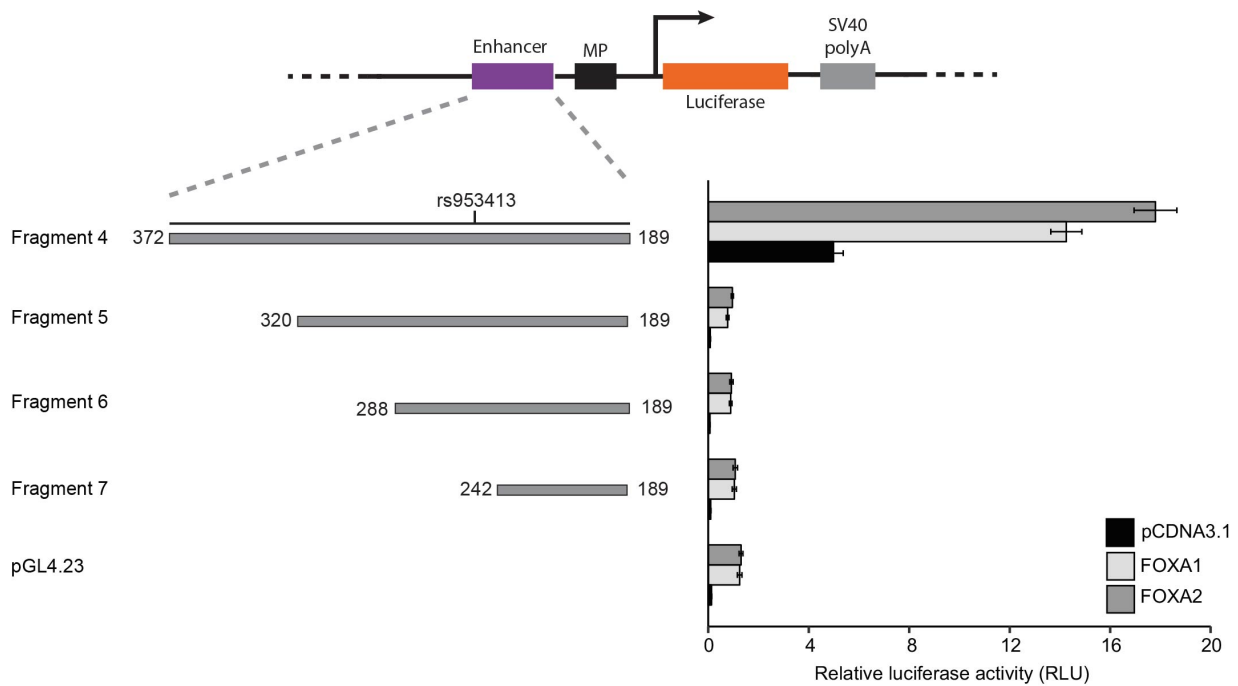


Figure S6. The whole ME element is essential for the enhancer activity of the rs953413 region induced by FOXA1 and FOXA2. Related to Figure 3. Only luciferase construct contains the whole ME element (Fragment 4) could be induced by FOXA1 and FOXA2 overexpression. Error bars, s.d. $n = 6$ from two independent plasmid extractions and transfections with each transfection had three technical replicates.

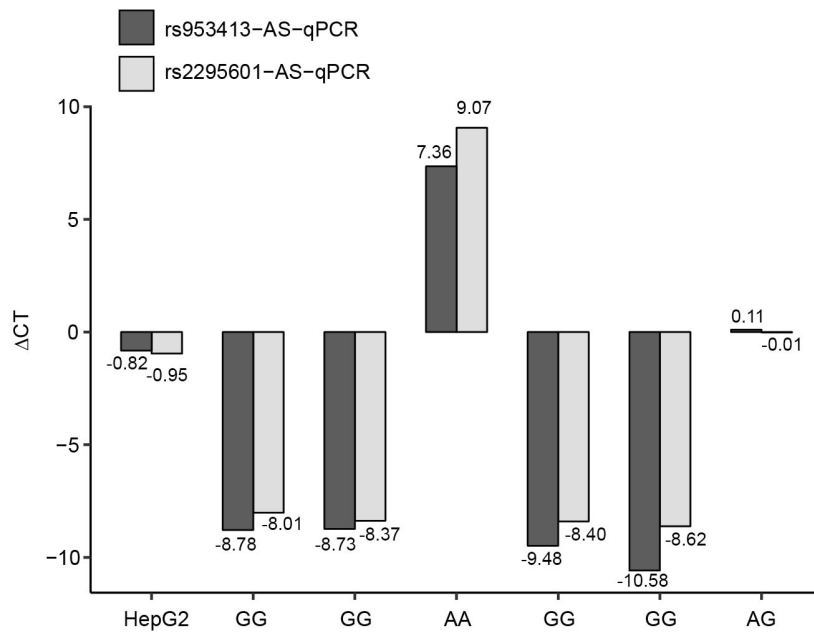


Figure S7. Validation of AS-qPCR primers for rs953413 and rs2295601 with genomic DNA from different samples as templates. Related to Figure 3-6. The y axis shows the C_T value differences in qPCR with different genomic DNA as templates for both rs953413[G] versus rs953413[A] (dark grey bar) and rs2295601[G] versus rs2295601[A] (light grey bar). The exact ΔC_T values are displayed for each experiment. The determined genotypes for both rs953413 and rs2295601 are the same in each sample and are listed on x axis. Due to existence of two copies of the G allele in HepG2 cells, the ΔC_T values in HepG2 cells for both SNPs are different from the normal heterozygous sample.

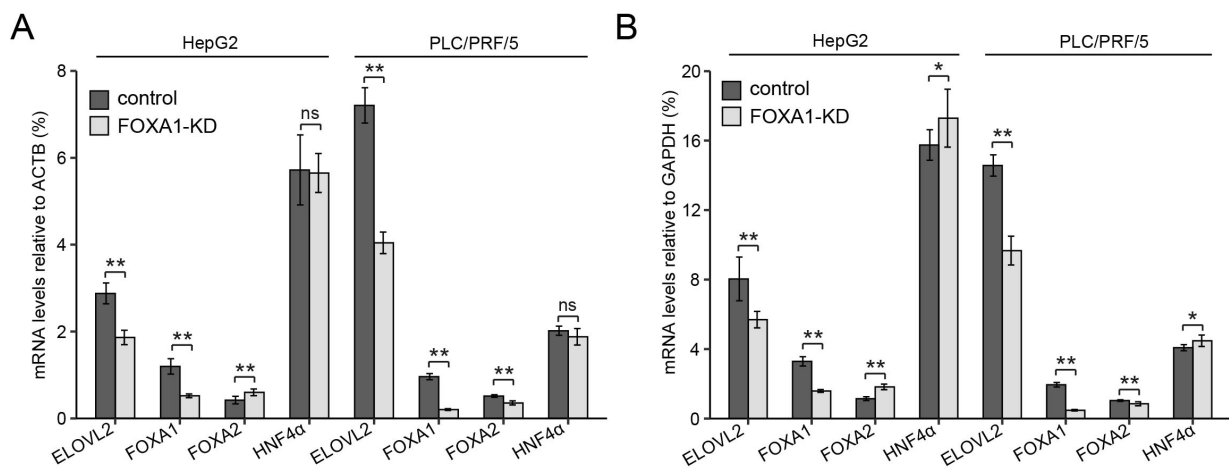


Figure S8. The expression of *ELOVL2* is significantly decreased by *FOXA1* knockdown. Related to Figure 3. The relative expression of each target gene was normalized with the expression of *ACTB* (A) and *GAPDH* (B). * $P < 0.05$; ** $P < 0.01$ and ns, not significant calculated by two-tailed Student's *t* tests. Error bars, s.d. $n = 8$ technical replicates from two independent experiments with each experiment had four replicates.

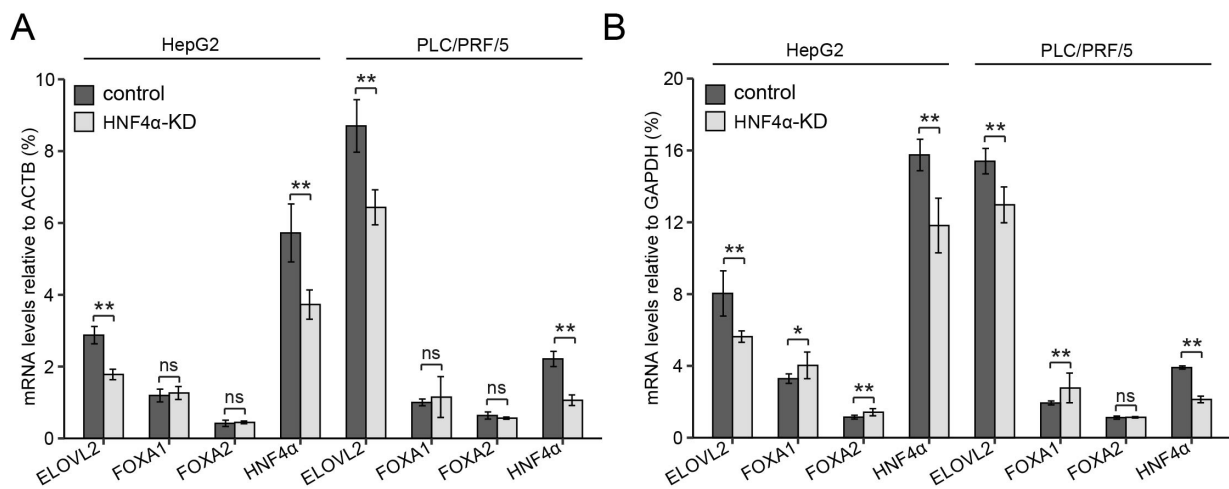


Figure S9. The expression of *ELOVL2* is significantly decreased by *HNF4α* knockdown. Related to Figure 4. The relative expression of each detected gene was normalized with the expression of *ACTB* (A) and *GAPDH* (B). * $P < 0.05$; ** $P < 0.01$ and ns, not significant calculated by two-tailed Student's *t* tests. Error bars, s.d. $n = 8$ technical replicates from two independent experiments with each experiment had four replicates.

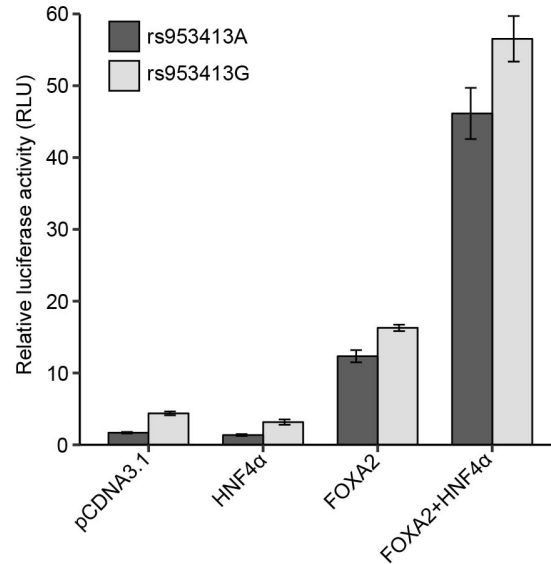


Figure S10. Cooperation between HNF4 α and FOXA2 significantly increased the enhancer activity of the rs953413 region in luciferase assay. Related to Figure 5. The enhancer activity of the rs953413 region is significantly increased by simultaneous overexpression of HNF4 α and FOXA2 compared with overexpression only HNF4 α or FOXA2 in luciferase assay. Error bars, s.d. $n = 6$ technical replicates from two independent plasmid extractions and transfections with each transfection had three technical replicates.

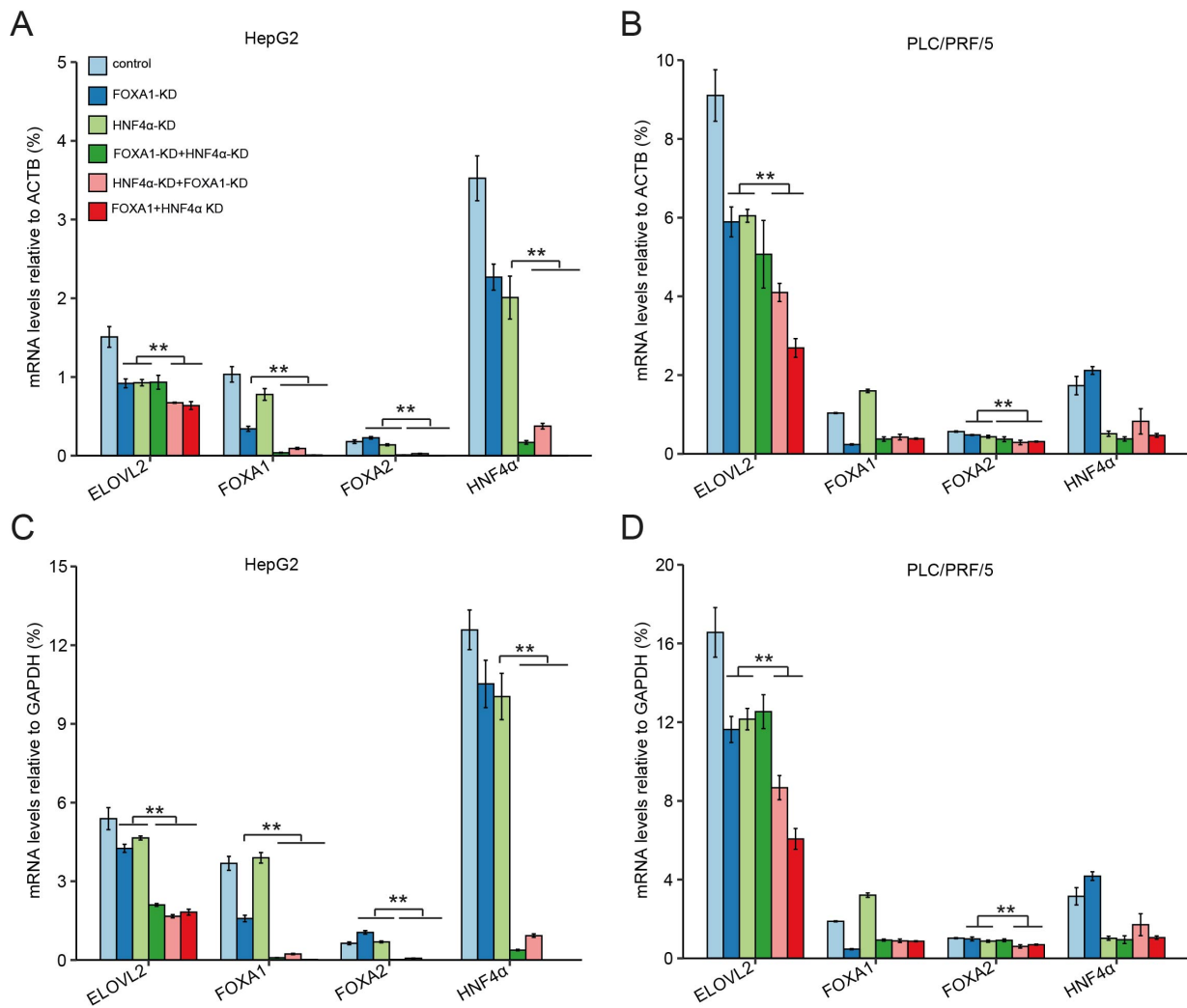


Figure S11. Double knockdown of both *HNF4α* and *FOXA1* leads to a significant decrease in *ELOVL2* expression compared with knockdown only *HNF4α* or *FOXA1*. Related to Figure 5. The relative expression of each gene is normalized to the expression of *ACTB* (A, B) and *GAPDH* (C, D) in both HepG2 and PLC/PRF/5 cells. The double knockdown cell lines were generated by either sequential or simultaneous lentivirus transduction. FOXA1-KD+HNF4α-KD denotes the cell line first transduced with the virus for *FOXA1* knockdown and then transduced the virus for *HNF4α* knockdown and vice versa for HNF4α-KD+FOXA1-KD. FOXA1+HNF4α KD denotes the cell line with simultaneously transduced virus for both *HNF4α* and *FOXA1* knockdown. ** $P < 0.01$ calculated by two-tailed Student's *t* tests. Error bars, s.d. $n = 4$ technical replicates.

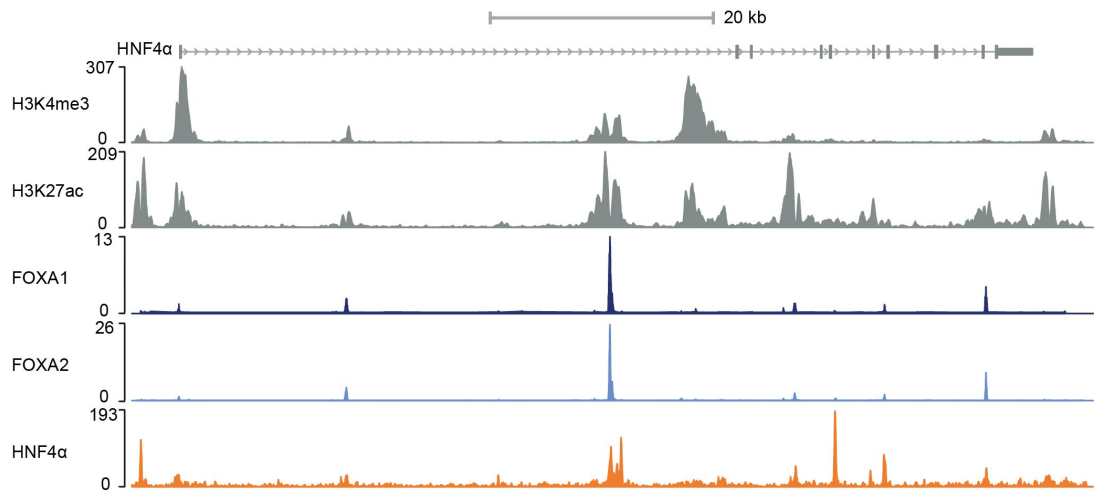
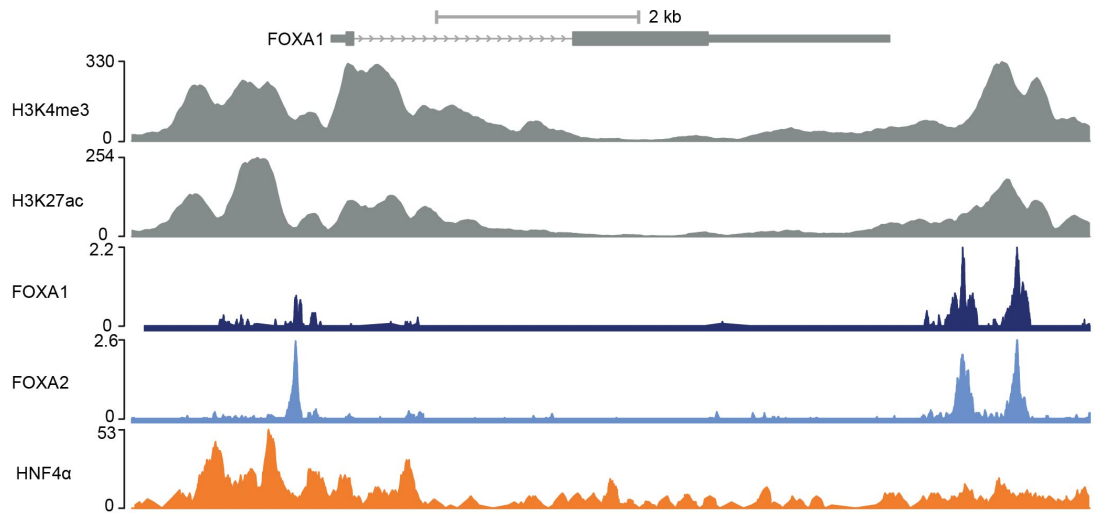
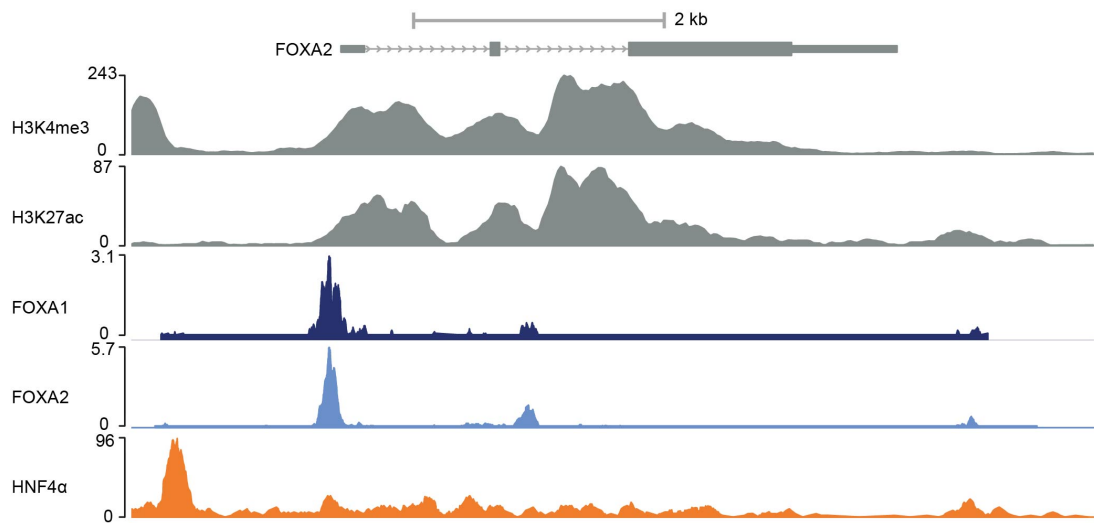
A**B****C**

Figure S12. ChIP-seq signals of HNF4 α , FOXA1 and FOXA2 from the ENCODE project are all enriched over the gene body of *HNF4 α* , *FOXA1* and *FOXA2*, respectively in HepG2 cells. Related to Figure 5. The ChIP-seq signals of HNF4 α , FOXA1 and FOXA2 together with H3K27ac and H3K4me3 signals in HepG2 cells are displayed over the gene body of *HNF4 α* (A), *FOXA1* (B) and *FOXA2* (C).

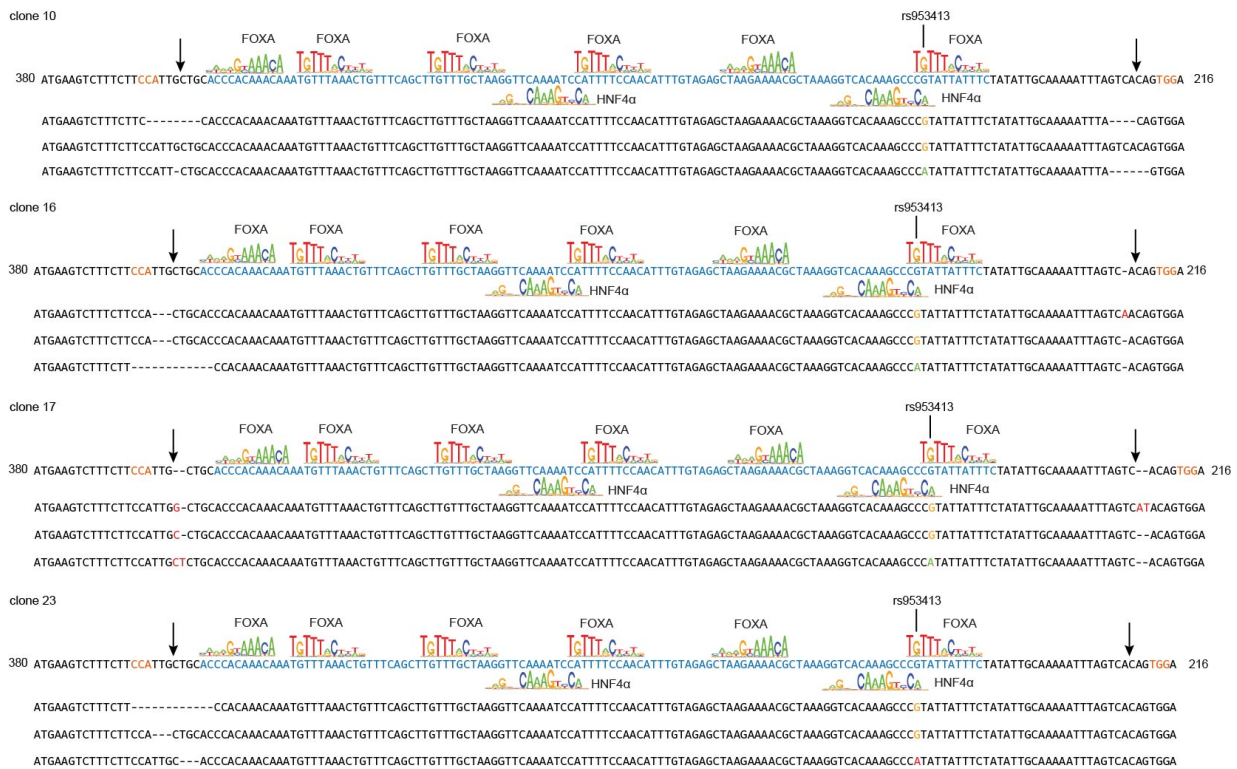


Figure S13. Individual clones bearing no mutations to the ME element identified by Sanger sequencing. Related to Figure 6. For each clone, genomic DNA was PCR-amplified and subjected to both direct PCR product sequencing and TA cloning sequencing. The ME element is highlighted in blue. The arrow denotes the expected Cas9 cut sites. Base-pair changes are shown in red and deletions are represented by dashes.

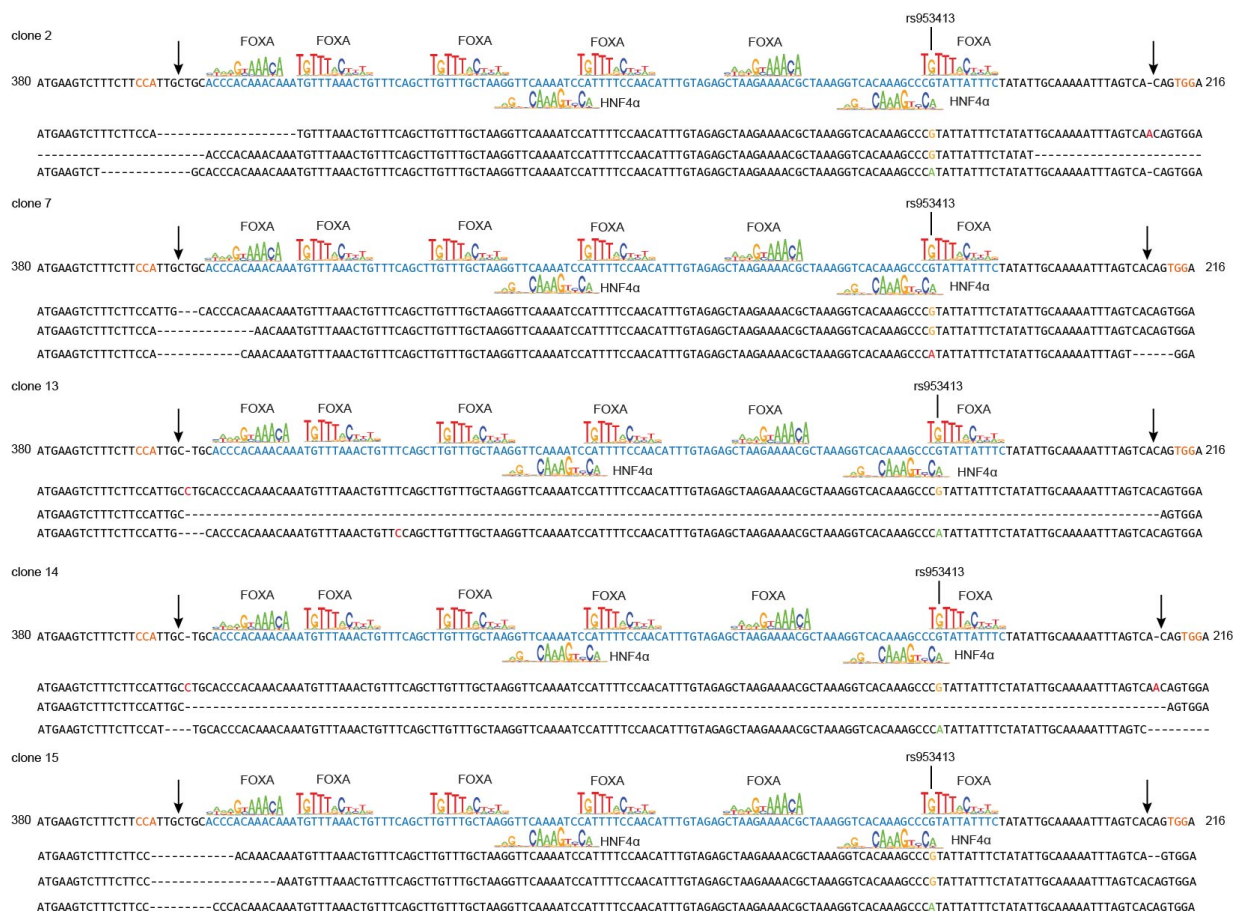


Figure S14. Individual clones with mutations introduced to one copy of the ME element bearing the G allele of rs953413 identified by Sanger sequencing. Related to Figure 6. For each clone, genomic DNA was PCR-amplified and subjected to both direct PCR product sequencing and TA cloning sequencing. The ME element is highlighted in blue. The arrow denotes the expected Cas9 cut sites. Base-pair changes are shown in red and deletions are represented by dashes.

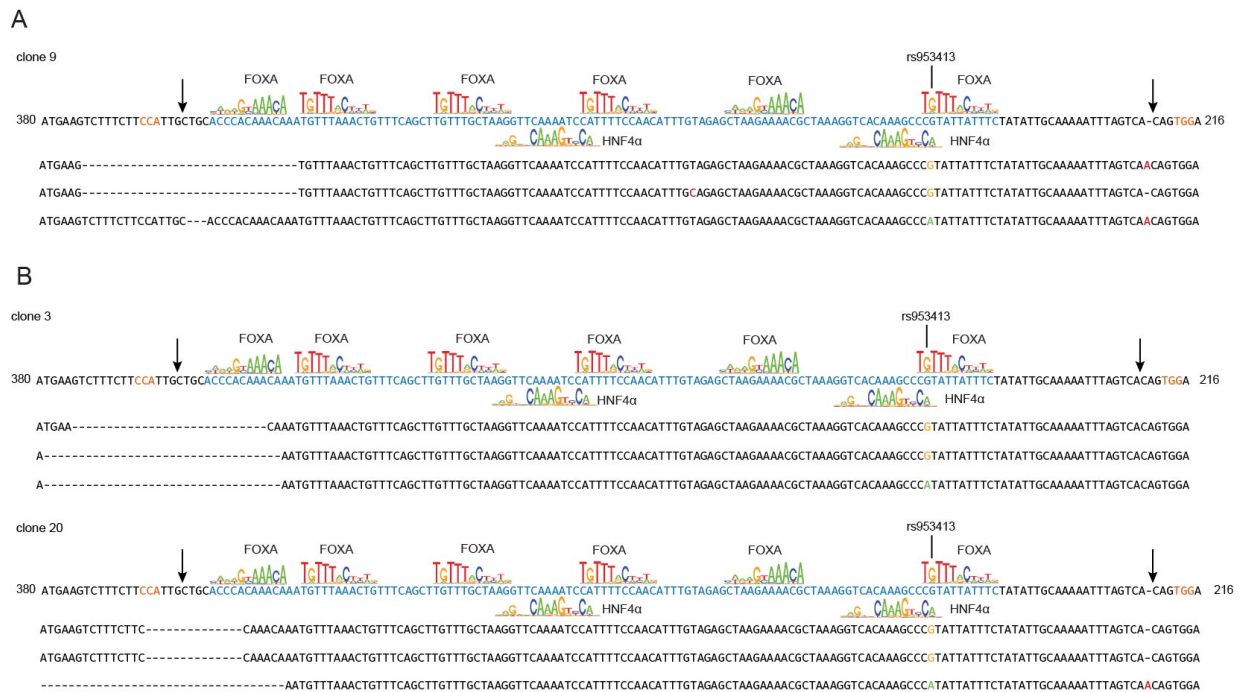


Figure S15. Individual clones with mutations introduced to multiple copies of the ME element identified by Sanger sequencing. Related to Figure 6. (A) clone 9 introduced mutations to both copies of the ME element bearing the G allele of rs953413. (B) clone 3 and clone 20 are verified to have mutations to all copies of the ME element. For each clone, genomic DNA was PCR-amplified and subjected to both direct PCR product sequencing and TA cloning sequencing. The ME element is highlighted in blue. The arrow denotes the expected Cas9 cut sites. Base-pair changes are shown in red and deletions are represented by dashes.

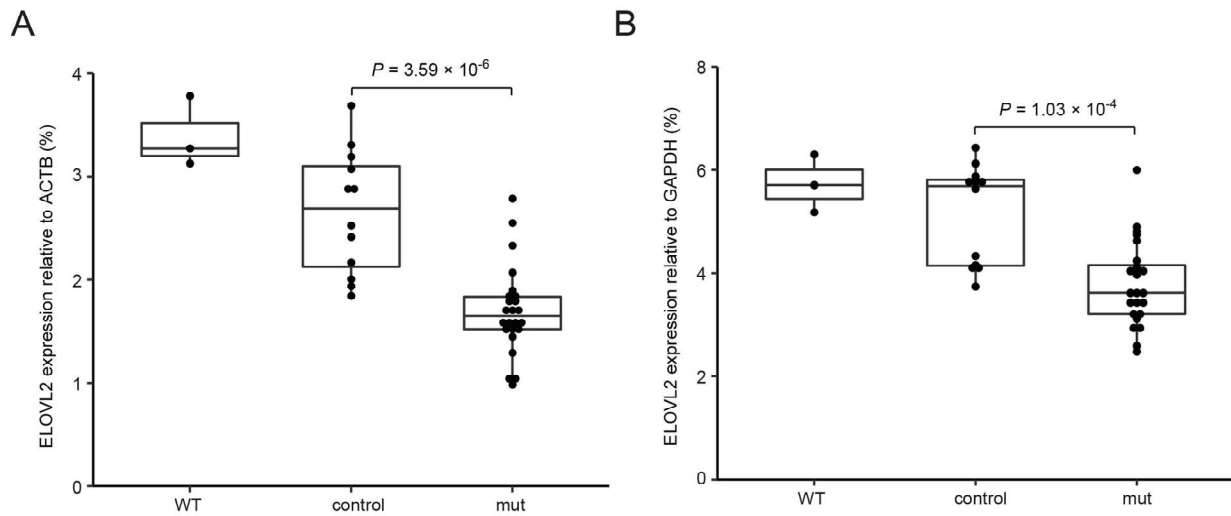


Figure S16. The clones bearing mutations in the ME element (mut) had impaired *ELOVL2* expression compared with clones without mutations introduced in the ME element (control).

Related to Figure 6. The expression of *ELOVL2* is either normalized to the expression of *ACTB* (A) or *GAPDH* (B). Each clone has three technical replicates. *P* values were evaluated using two-tailed Student's *t* tests. WT denotes *ELOVL2* expression from normal HepG2 cells ($n=3$).

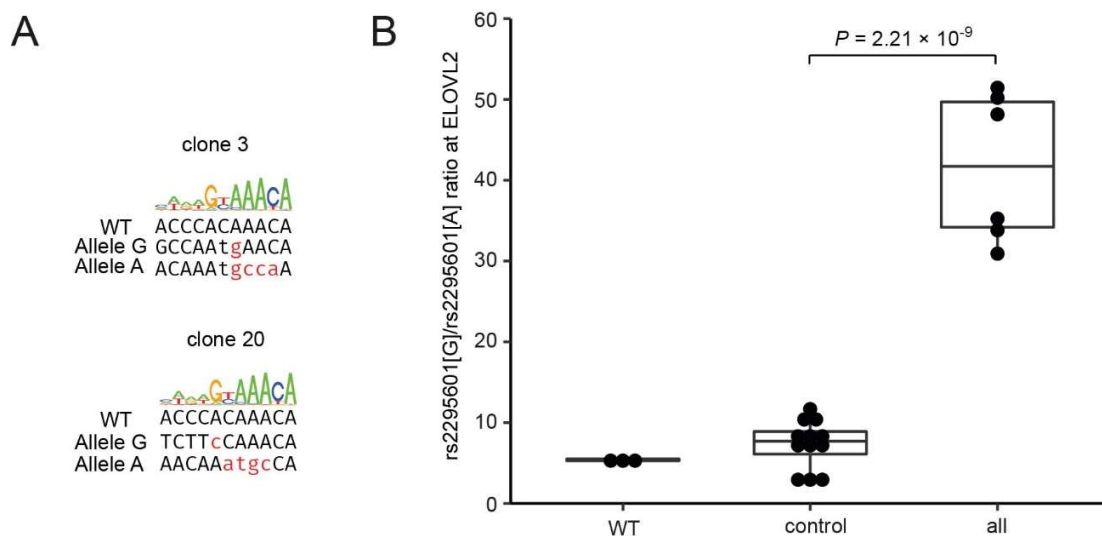


Figure S17. Increased allelic imbalance in *ELOVL2* expression in clone 3 and clone 20. Related to Figure 6. (A) In both clone 3 and clone 20, the ME element of each allele is mutated and the ME elements bearing the G allele of rs953413 have a more conserved FOXA motif compared to the A allele (see also Figure S15B). WT represents the wild type sequence while allele G and allele A represent the mutated ME sequences in linkage with rs953413[G] and rs953413[A], respectively. The mutated key motif sequences are displayed in lower-case letters and highlighted in red. (B) The increased allelic imbalance in *ELOVL2*

expression is detected by rs2295601 AS-qPCR. A significant increase in allelic imbalance of *ELOVL2* expression is observed in clone 3 and clone 20 (all) when compared with clones without mutations introduced to the FOXA motif (control, as listed in Figure S13). WT represents the observed allelic imbalance in *ELOVL2* expression in normal HepG2 cells ($n=3$).

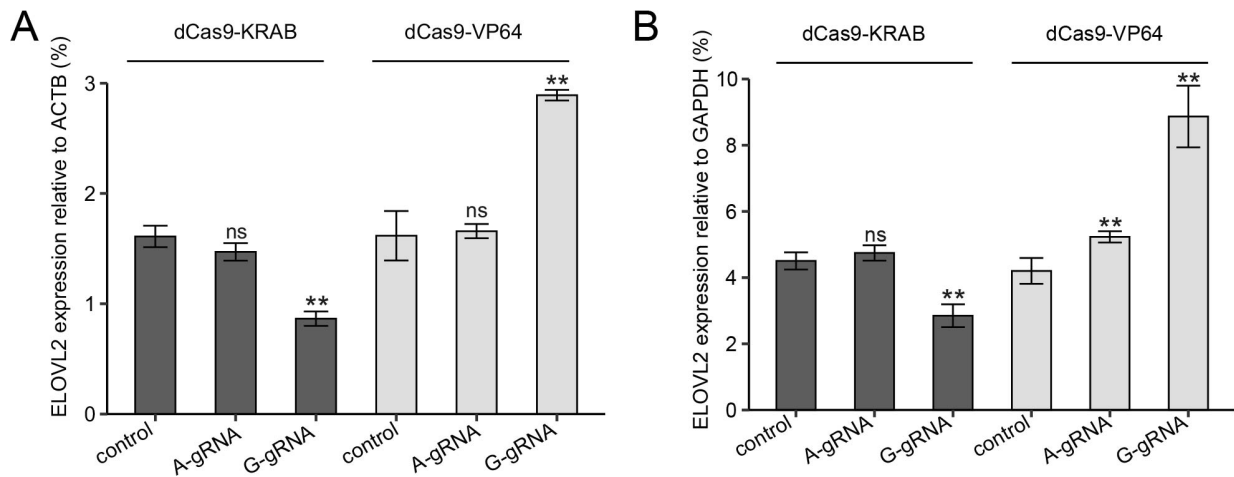


Figure S18. The effect of AS-gRNA targeting rs953413 coupled with dCas9-effector on *ELOVL2* expression. Related to Figure 6. The expression of *ELOVL2* was normalized to the expression of *ACTB* (A) and *GAPDH* (B), respectively. HepG2 cells transduced with only dCas9-effector virus was employed as the control. ** $P < 0.01$ and ns, not significant calculated by two-tailed Student's *t* tests. Error bars, s.d. $n = 4$ technical replicates.

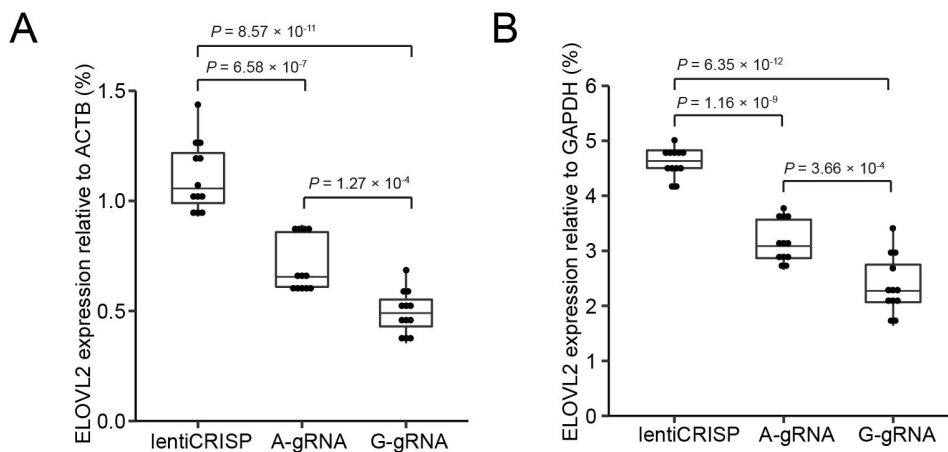


Figure S19. The expression of *ELOVL2* was significantly decreased by mutations introduced to rs953413 by AS-gRNA targeting rs953413 coupled with wide type Cas9. Related to Figure 6. The

expression of *ELOVL2* was normalized to the expression of *ACTB* (A) and *GAPDH* (B). The expression of *ELOVL2* in HepG2 cells transduced with lentiCRISP v2 virus was used as the control. $n = 12$ technical replicates. The P values were calculated by two-tailed Student's t tests.

Supplemental Tables

Table S3. AS-SNPs in the *ELOVL2* locus. Related to Figure 1.

SNP	allele	AF (EUR)	FOXA1 (sc101058)		FOXA1 (sc6553)		FOXA2 (sc6554)	
			Rep 1	Rep 2	Rep1	Rep2	Rep1	Rep2
rs953413	rs953413[G]	0.56	22	12	15	15	4	28
	rs953413[A]	0.44	5	4	14	4	1	9
rs3798713	rs3798713[G]	0.58	10	11	17	4	NA	16
	rs3798713[C]	0.42	2	1	5	3	NA	2
rs17675073	rs17675073[G]	0.86	0	2	3	1	NA	2
	rs17675073[A]	0.14	9	9	13	2	NA	4

Note: The number of uniquely mapped reads covering each allele in ChIP-seq was reported for each AS-SNP. NA, no reads covered. AF, allele frequency in European population.

Transparent Methods

Allelic imbalance in chromatin binding of the rs953413 and rs3798713 region in ChIP-seq experiments

The bam files for each TF mapped to regions where AS-SNPs are located were acquired from the ENCODE project (The Encode Project Consortium, 2012). Duplicate reads were removed with picard MarkDuplicates (<http://broadinstitute.github.io/picard>). Aligned reads with mismatch other than the SNP were discarded with bamtools (Barnett et al., 2011). The reads mapped to each allele were separated with splitSNP (<https://github.com/astatham/splitSNP>) and counted.

Expression plasmids construction

The human *FOXA1* gene was amplified from HepG2 cDNA and cloned into pCDNA3.1 through SLiCE cloning method (Zhang et al., 2012). The ORF clone of *FOXA2* was purchased from Sino Biological (HG14174-G). Plasmid pCDNA3.1-*FOXA2* was constructed by inserting the coding region of *FOXA2* into pCDNA3.1 digested with HindIII and EcoRV through SLiCE cloning method (Zhang et al., 2012). FR_HNF4A2 was a gift from Gerhart Ryffel (Addgene plasmid # 31100) (Thomas et al., 2004). Plasmid

pCDNA3.1-HNF4 α was constructed by inserting the coding sequence of *HNF4 α* isoform 2 digested with KpnI and NotI from FR_HNF4A2 into pCDNA3.1 digested with the same enzymes. All the plasmids are validated by Sanger sequencing. The detailed primer sequences for each expression construct is listed in Table S5.

Luciferase constructs and reporter assay

Plasmid pSV40 was constructed by transfer the SV40 promoter sequence from pGL3-promoter vector into pGL4.10 (Promega) through BglII and HindIII double digestion. The 287-bp (chr6: 11,008,440-11,008,726; hg19) fragment containing both rs3798713 and rs17675073 was used for enhancer validation. The 529-bp (chr6: 11,012,583-11,013,111; hg19) rs953413-centered region was also selected for enhancer validation based on the ChIP-seq signals for different TFs from the ENCODE project (Figure S4). The regions were amplified from HepG2 genomic DNA and inserted upstream of either the minimal promoter (MP) sequence of pGL4.23 (Promega) or the SV40 promoter sequence of pSV40 to test their enhancer activities. To identify the ME region encompassing rs953413, a series of truncation and deletion luciferase constructs were generated by SLiCE cloning method (Zhang et al., 2012). A three fragments In-fusion cloning system (Takara) with mutations introduced through primer sequences was employed to introduce desired mutations into luciferase constructs. The detailed primer information and cloning method for each construct is listed in Table S4. All the resulting plasmids were verified by Sanger sequencing.

HepG2 cells were plated one day before transfection in 96-well plates. The confluency was 50-70% on transfection. For normal luciferase assay, each well was transfected with 0.3 μ l X-tremeGENE HP DNA transfection reagent (Roche) and 100 ng of experimental firefly luciferase reporter plasmid, and 1 ng of pGL4.74 renilla luciferase reporter vector as internal control for monitoring transfection and lysis efficiency. For luciferase assay overexpressing HNF4 α in Figure 4A and 4B, each well was transfected with 0.3 μ l X-tremeGENE HP DNA transfection reagent (Roche), 40 ng of firefly luciferase reporter plasmid, 50 ng pCDNA3.1-HNF4 α and 10 ng of pRL-MP described earlier (Pan et al., 2017). For other cotransfection experiments, each well was transfected with 0.3 μ l X-tremeGENE HP DNA transfection reagent (Roche), 50 ng of firefly luciferase reporter plasmid, 50 ng of expression plasmid and 1 ng of pGL4.74. For experiments cotransfecting HNF4 α and FOXA1 in Figure 5A and cotransfecting HNF4 α and FOXA2 in Figure S10, 25 ng of each expression plasmid was used with plasmid pCDNA3.1 used as control.

Cells were harvested 24 h after transfection and assayed with the Dual-Luciferase Reporter Assay System (Promega) on an Infinite M200 pro reader (Tecan). All the results are expressed directly as the ratio of firefly luciferase activity from experiment plasmids to renilla luciferase activity from control plasmids. All the luciferase experiments came from two independent transfections i.e., independent plasmid preparations and transfections each with three technical replicates. Luciferase values are expressed as

averages with error bars representing standard deviations (s.d) from all technical replicates and statistical analyses were performed by two-tailed Student's *t* tests.

Cell culture

HepG2 cells were originally purchased from the American Type Culture Collection (ATCC) and maintained in RPMI1640 basal medium supplemented with 10% fetal bovine serum (FBS) and 2 mM L-glutamine. Human PLC/PRF/5 cells were purchased from European Collection of Authenticated Cell Cultures (ECACC 85061113) and maintained in high glucose DMEM medium supplemented with 10% FBS, 1 mM sodium pyruvate. 293T cells were grown in DMEM supplemented with 10% FBS, 1 mM sodium pyruvate, and 500 µg/ml Geneticin. All the cells were also supplemented with 100 units of penicillin and 100 µg of streptomycin per 1 ml of culture medium.

Lentiviral-mediated gene knockdown

Both shRNA and artificial miRNA expression cassettes were utilized to knockdown target genes. The shRNA sequence was directly synthesized and inserted into pGreenPuro shRNA expression lentivector (SI505A-1, System Biosciences) digested with BamHI and EcoRI. The artificial miRNA precursor was constructed from the natural miR-124-1 precursor sequence introducing two suitable restriction sites recognized by EcoRV and EcoRI, respectively (Liang et al., 2012). The constructed artificial miRNA precursor was inserted downstream of the puromycin resistance gene through SLiCE cloning method. The target sequences for *FOXA1* knockdown are GATGTGTAGACATCCTCCGTATATT and GGCGTACTACCAAGGTGTGTA. For *HNF4α* knockdown, the target sequences are GAACCACATGTACTCCTGCAGATT and TCAGCACTCGAAGGTCAAGCTAT. The detailed primer information for each lentiviral construct is listed in Table S5.

Lentivirus was produced in 293T cells by transfecting the lentiviral plasmid together with packaging plasmids pLP1, pLP2 and envelope plasmid pLP/VSVG (Life Technologies) using polyethylenimine (Polysciences) following the manufacturer's instructions. Cells were plated in 24-well plates and transduced with virus supernatant together with sequabrene (Sigma) at final concentration of 8 µg/ml. The cell lines with double knockdown of *FOXA1* and *HNF4α* were achieved by sequential or simultaneous transduction of virus knocking down *FOXA1* and *HNF4α*. The cell lines with target gene knockdown were selected by puromycin (Life Technologies) at concentration of 1 µg/ml for HepG2 cells and 4 µg/ml for PLC/PRF/5 cells. The selected cells were maintained with 0.5 µg/ml of puromycin and regularly passaged for further analysis.

Quantitative real time PCR

At least three replicates were studied by quantitative real time PCR (qPCR) on cDNA samples and on genomic DNA samples from ChIP experiments. List of primers used in this study is shown in Table S6. The qPCR reactions were performed with JumpStart Taq ReadyMix (Sigma) coupled with EvaGreen dye (Biotium). For gene expression analysis, equal number of cells (8×10^5 for HepG2 cells and 2.5×10^5 for PLCR/PRF/5 cells) were plated in 12-well plates 24 h before harvesting. Total RNA was extracted from cells with TRIzol (Life Technologies) according to the manufacturer's instructions. A total of 1 μ g total RNA was reverse transcribed into cDNA with Maxima First Strand cDNA synthesis kit (Life Technologies). The expression was normalized to three control transcripts including *RSP18*, *ACTB* and *GAPDH*. Statistical analyses were carried out by two-tailed Student's *t* tests.

For ChIP experiments, a standard curve was generated for each target with serial-diluted input DNA as templates. The amounts of DNA pulled down for each target was first normalized to the input based on the standard curve. Then the relative enrichment of target DNA was displayed as fold changes over the negative control region GDCHR12, located in one gene desert region on chromosome 12. The promoter region of *HNF1 α* (HNF1 α -pro) was used as the positive control. All the primer sequences used for qPCR analysis are listed in Table S6.

Allele-specific quantitative PCR

Primers for AS-qPCR were designed based on mismatch amplification mutation assay (MAMA) to accurately quantify single nucleotide mutations (Cha et al., 1992; Li et al., 2004). Allele-specific amplification of the rs953413 region was employed to validate the allelic imbalance in chromatin binding of both TFs and H3K27ac in ChIP experiments. The exonic rs2295601 AS-qPCR was used to evaluate the allelic imbalance in *ELOVL2* expression. The PCR reactions were carried out with JumpStart Taq ReadyMix (Sigma) coupled with EvaGreen dye (Biotium). The specificity of the AS-qPCR primers was validated with genomic DNA from different samples as templates from the Excellence of Diabetes Research in Sweden (EXODIAB) biobank and shown in Figure S7. The detailed primer sequences used in AS-qPCR are listed in Table S6.

Chromatin immunoprecipitation

ChIP experiments were carried out as previously described with modifications (Blecher-Gonen et al., 2013; Pan et al., 2017). Cells were cultured in T175 flask until reaching confluency of >80% and crosslinked with 1% formaldehyde on a shaking platform for 10 min at room temperature and quenched with 125 mM glycine for 5 min. Cells were collected, washed twice with ice-cold PBS and resuspended in cell lysis buffer (10 mM Tris-HCl, pH 8.0, 10 mM NaCl and 0.2% NP-40) supplemented with protease inhibitor (Roche) to isolate nuclei. RIPA buffer (1 \times PBS, 1%NP-40, 0.1% SDS, 0.5% sodium deoxycholate and 0.004% sodium azide) supplemented with protease inhibitor was used to isolate the cross-linked

chromatin from nuclei. The isolated chromatin was sonicated to an average size of 250 bp using the Bioruptor Pico sonication device (Diagenode). An aliquot was saved each time to be subjected to DNA extraction and used as input. The leftover was used for ChIP assay.

For ChIP experiments with antibody against histone modification H3K27ac, 4 µg of antibody from Abcam (ab4729) together with 40 µl of Dynabeads protein G (Life Technologies) was added simultaneously into sonicated chromatin from 1×10^6 cells and incubated on a rotating platform overnight at 4°C. For ChIP experiments against TFs, chromatin from 3×10^6 cells was first precleared by incubating with 30 µl Dynabeads for 2 h at 4°C. The supernatant was separated and incubated overnight at 4°C with 8 µg of antibody against FOXA1 (ab5089, Abcam), FOXA2 (SC-6554 for HepG2 and SC-374376 for PLC/PRF/5 due to discontinuation of antibody used in HepG2 cells, Santa Cruz Biotechnology) or HNF4α (SC-6556X for HepG2 cells and SC-374229 for PLC/PRF/5 due to discontinuation of antibody used in HepG2 cells, Santa Cruz Biotechnology). Normal rabbit IgG (12-370, Millipore) was also included to check the background of antibody nonspecific binding in each batch of experiments. The immune complexes were captured by incubation with 75 µl of Dynabeads protein G at room temperature for 1 h. For all ChIP assays, a series of washing steps was applied to Dynabeads protein G after immunoprecipitation including four times of washing with RIPA buffer, two times of washing with ChIP wash buffer (10 mM Tris-HCl, pH 8.0, 0.25 M LiCl, 10 mM EDTA, 1% NP-40 and 1% sodium deoxycholate) and once with TE buffer. The DNA-protein complexes were eluted in direct elution buffer (10 mM Tris-HCl, pH 8.0, 5 mM EDTA, 0.3 M NaCl and 0.5% SDS) and together with the previous saved sonicated lysates to be used as input were treated with RNase A and proteinase K respectively and incubated at 65°C overnight to reverse crosslink. DNA was purified with Agencourt AMPure XP beads (Beckman Coulter) following the manufacturer's instructions, eluted in 10 mM Tris-HCl (pH 8.0) and ready to be analyzed by qPCR. Input DNA was quantified by Nanodrop 2000 (Life Technologies) and serially diluted to be used as templates for setting up standard curves of different primers targeting candidate regions.

CRISPR/Cas9-mediated genome editing

Lentivector lentiCRISPR v2 (Addgene plasmid # 52961) was a gift from Feng Zhang (Sanjana et al., 2014). In order to knock out the ME element, two gRNAs adjacent to the ME element were designed. The expression of the two gRNAs are driven by human and mouse U6 promoter, respectively. The expression cassette is inserted in lentiCRISPR v2 digested with BsmBI by In-Fusion cloning system (Takara). The AS-gRNA targeting each allele of rs953413 was directly synthesized and inserted into lentiCRISPR v2 digested with BsmBI through T4 ligation. The identity of all the constructs were validated by Sanger sequencing. The detailed primer information is listed in Table S5. The lentivirus was produced in 293T cells and transduced into HepG2 cells coupled with sequabrene (Sigma) at final concentration of 8 µg/ml in 12-well plate. The positive cells were selected by puromycin (Life Technologies) at concentration of 1 µg/ml. Individual colonies were generated by splitting the positive cells to 0.5~3 cells per well in 96-well

plates and culturing in normal medium until single colony is formed. The genomic DNA for each single colony in 96-well plate is extracted by QuickExtract DNA Extraction Solution (QE09050, Lucigen). The introduced mutations for each colony are verified by both direct PCR sequencing and TA cloning followed by Sanger sequencing with the primers listed in Table S6. The selected colonies are passed regularly until reaching T75 flask and ready for expression study.

Transactivation and transrepression of the rs953413 locus through dCas9-effector coupled with rs953413 AS-gRNA

Lentiviral plasmid lenti-EF1a-dCas9-KRAB-Puro (Addgene plasmid # 99372), lenti-EF1a-dCas9-VP64-Puro (Addgene plasmid # 99371) and lentiGuide-Hygro-eGFP (Addgene plasmid # 99375) were gifts from Kristen Brennand (Ho et al., 2017). The AS-gRNA targeting each allele of rs953413 was directly synthesized and inserted into lentiGuide-Hygro-eGFP digested with BsmBI through T4 ligation. The HepG2 cells stably expressing dCas9-KRAB and dCas9-VP64 were acquired by lentiviral transduction followed by puromycin selection at 1 µg/ml. The cells expressing dCas9-effector were further transduced with lentivirus expressing AS-gRNA targeting either the A allele or the G allele of rs953413 and selected with medium containing 1 µg/ml puromycin and 0.2 mg/ml of hygromycin B (Life Technologies) until ready for expression study.

Supplemental References

Barnett, D.W., Garrison, E.K., Quinlan, A.R., Strömberg, M.P., and Marth, G.T. (2011). BamTools: a C++ API and toolkit for analyzing and managing BAM files. *Bioinformatics* 27, 1691-1692.

Battle, A., Brown, C.D., Engelhardt, B.E., and Montgomery, S.B. (2017). Genetic effects on gene expression across human tissues. *Nature* 550, 204-213.

Blecher-Gonen, R., Barnett-Itzhaki, Z., Jaitin, D., Amann-Zalcenstein, D., Lara-Astiaso, D., and Amit, I. (2013). High-throughput chromatin immunoprecipitation for genome-wide mapping of in vivo protein-DNA interactions and epigenomic states. *Nat Protoc* 8, 539-554.

Cha, R.S., Zarbl, H., Keohavong, P., and Thilly, W.G. (1992). Mismatch amplification mutation assay (MAMA): application to the c-H-ras gene. *PCR Methods Appl* 2, 14-20.

Ho, S.M., Hartley, B.J., Flaherty, E., Rajarajan, P., Abdelaal, R., Obiorah, I., Barretto, N., Muhammad, H., Phatnani, H.P., Akbarian, S., *et al.* (2017). Evaluating Synthetic Activation and Repression of Neuropsychiatric-Related Genes in hiPSC-Derived NPCs, Neurons, and Astrocytes. *Stem cell reports* 9, 615-628.

Lemaitre, R.N., Tanaka, T., Tang, W., Manichaikul, A., Foy, M., Kabagambe, E.K., Nettleton, J.A., King, I.B., Weng, L.-C., Bhattacharya, S., *et al.* (2011). Genetic Loci Associated with Plasma Phospholipid n-3 Fatty Acids: A Meta-Analysis of Genome-Wide Association Studies from the CHARGE Consortium. *PLoS Genet* 7, e1002193.

Li, B., Kadura, I., Fu, D.-J., and Watson, D.E. (2004). Genotyping with TaqMAMA. *Genomics* 83, 311-320.

Liang, G., He, H., Li, Y., and Yu, D. (2012). A new strategy for construction of artificial miRNA vectors in *Arabidopsis*. *Planta* 235, 1421-1429.

Pan, G., Ameer, A., Enroth, S., Bysani, M., Nord, H., Cavalli, M., Essand, M., Gyllensten, U., and Wadelius, C. (2017). PATZ1 down-regulates FADS1 by binding to rs174557 and is opposed by SP1/SREBP1c. *Nucleic Acids Res* 45, 2408-2422.

Sanjana, N.E., Shalem, O., and Zhang, F. (2014). Improved vectors and genome-wide libraries for CRISPR screening. *Nat Methods* 11, 783-784.

The Encode Project Consortium (2012). An integrated encyclopedia of DNA elements in the human genome. *Nature* 489, 57-74.

Thomas, H., Senkel, S., Erdmann, S., Arndt, T., Turan, G., Klein-Hitpass, L., and Ryffel, G.U. (2004). Pattern of genes influenced by conditional expression of the transcription factors HNF6, HNF4alpha and HNF1beta in a pancreatic beta-cell line. *Nucleic Acids Res* 32, e150.

Zhang, Y., Werling, U., and Edelmann, W. (2012). SLiCE: a novel bacterial cell extract-based DNA cloning method. *Nucleic Acids Res* 40, e55-e55.